Investigation of the zero resistance and temperature-dependent superconductivity phase transition in Pb-Cu-P-S-O compound

Huk Geol Kim[1], Dae Cheol Jeong[2] and Hyun-Tak Kim[3,*]

[1] *Independent Researcher, Seoul 06132, South Korea*

[2] *SuperConductor Technology LAB Corp. Ltd., Seoul 06132, South Korea*

[3] *Department of Physics, College of William & Mary, Williamsburg, VA 23185, USA*

*Corresponding author : Hyun-Tak Kim, hkim22@wm.edu

Abstract – In our previous study, we suggested a synthetic method for the replication of PCPOSOS ($Pb_{10-x}Cu_x[P(O_{1-y}S_y)_4]_6O_{1-z}S_z$) and showed precisely measured zero resistance. Through the synthesis method we named Daecheol-Mingi (DM) method, we measured the phenomenon of superconductivity phase transition depending on temperature. Also, we repeated validation of zero resistance of the samples. This paper presents a specific critical temperature for PCPOSOS, demonstrating consistency with the original authors' data.

Keywords – *superconductor, room temperature, ambient pressure, PCPOSOS.*

I. Introduction

Recently, PCPOSOS [1]($Pb_{10-x}Cu_x[P(O_{1-y}S_y)_4]_6O_{1-z}S_z$) (x= 3 ~6, y+z=0.3 ~ 0.4), which has garnered international attention, has been recognized as a potential room-temperature superconductor (RTSC). Although many research teams have attempted to replicate the it, they replicated PCPOO ($Pb_{10-x}Cu_x(PO_4)O$) (x= 0.9 ~1.1) which is the previously known chemical formula. Research teams concluded that PCPOO is an insulator. However, the possibility of superconductivity emerging from the lanakite structure has been suggested through DFT simulation[2]. Also, Kim [3] suggested that the superconductivity of PCPOSOS can be interpreted by BR-BCS theory. To date, unfortunately, only a few studies have seriously attempted to replicate PCPOSOS. However, the potential Meissner effect has been discovered by some research groups[4]. Furthermore, in our previous study, we repeatedly confirmed the zero resistance of PCPOSOS [5].

In this study, we focused on the phase transition depending on temperature, which is crucial evidence of superconductivity. We have repeatedly validated the phase transition and present the critical temperature. The estimated critical temperature aligns with the claims of the original authors [6]. Moreover, for those who may not understand despite the zero resistance data in our previous paper, we kindly provide additional explanations and reveal the RTSC mechanism.

II. Details of the synthesized samples

All samples were synthesized using the DM method, same to the approach suggested in the previous study[5]. The samples used in this study are samples #5 and 6, which already showed zero resistance [5], along with the newly synthesized sample #8. As shown in Fig. 1, the synthesized samples uniformly showed a coppery or dark-gray surface color. We already explained that the cross-section of the samples consistently appears with a silver-gray or dark-gray color. To measure the electrical characteristics of the samples, it is recommended to apply probes to the dark-gray or silver-gray areas. Table 1 shows the size of each sample.

(a) sample #5 (b) sample #6 (b) sample #8

Fig. 1. The shape and appearance of the synthesized samples.

Table 1. Size of the samples and copper plate.

	Length (mm)	Width (mm)	Thickness (mm)
Sample #5	17.0	13.0	4.0
Sample #6	17.0	14.0	3.0
Sample #8	16.1	14.2	4.4

III. Current (I) -Voltage (V) measurements

In the measurements, the used current source and voltage measurement equipment were the Keithley models 6221 and 2182A, respectively. The utilized 4-point probe station is M.S.Tech M4P302 model which uses gold-coated probes. We used the well-known four-probe method setting electrode distances of 1 mm. Fig. 2 shows the measured voltages of the sample #5 for applied current in the range of -100 to 100 mA. The fact that the measured voltages are already evaluated to be zero, because it is similar to the noise level of the equipment, and the slope (Resistance R=dV/dI) becomes zero on average. This indicates that the resistance is already zero in that applied current range. Pure metals and conductors do not exhibit this flat behavior. This behavior is also exhibited for sample#6 and 8 as well (Figs. 3 and 4) Moreover, we calculated a voltage of ΔV eliminating contact resistance and wire resistances as follows: $V \equiv \Delta V = \frac{V_+ - V_-}{2}$, where V_+ is a voltage in a positive current I_+ and V_- is a voltage in a negative current I_- (see Fig. 5).

As shown in Figs 2, and 3, all samples show zero resistances. The voltages are not proportional to the applied current (Ohmic behavior) in the range of -100 mA to 100 mA. This aligns precisely with the zero resistance observed in the previous research[5]. Additionally, we have repeatedly confirmed that the zero-resistance phenomenon did not occur when measuring copper plate and insulator for verification and validation of the measurement process and method. Furthermore, Fig. 5 clearly shows that the sample is in the condensed state for the entire range of applied current. Although the sample is inhomogeneous, the calculated average voltage being 0 indicates zero resistance, providing decisive evidence of the presence of a superconducting component or phase in the current channel. Fig. 4 shows microvolt voltages and hysteresis behaviors measured for sample #8. Moreover, it exhibits a phenomenon that voltage decreases with increasing current. The dependence of current is similar to the percolation phenomenon displayed in a semiconductor. Hysteresis phenomenon with current is depicted as well. A property crossing zero voltage appears, regarded as the zero resistance characteristic. The behaviors indicate that sample 8 has two kinds of phases such as zero-resistance phase and semiconducting phase. Sample #8 is different from samples #5 and 6.

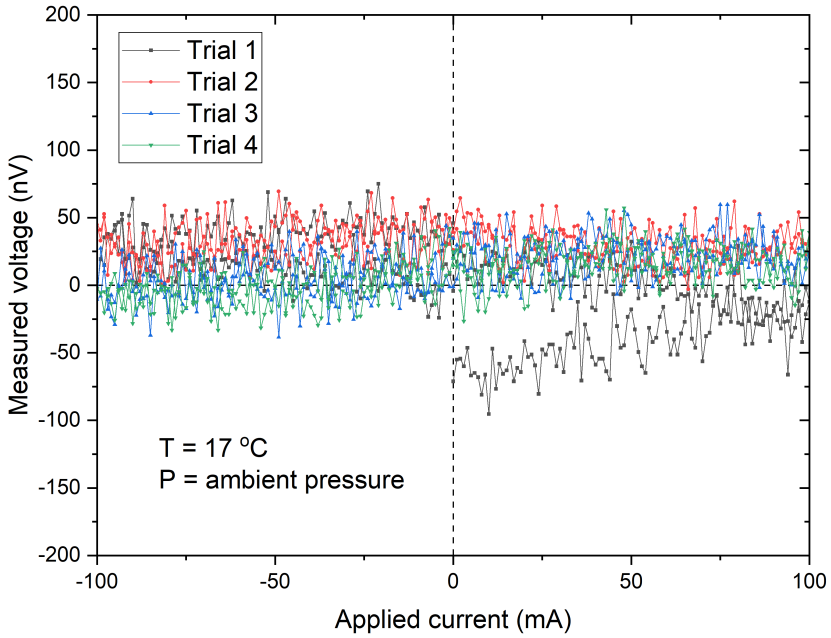

Fig. 2. Measured voltages for applied current ranging from -100 mA to 100 mA (sample #5), (newly measured data), The averaged slope dV/dI =Resistance=0 is evaluated, which indicates that resistance is zero.

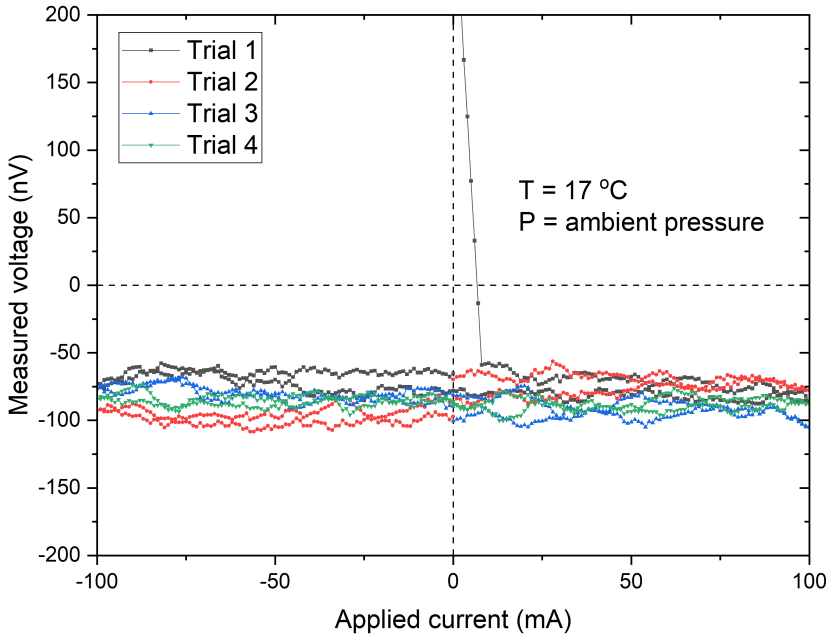

Fig. 3. Measured voltages for applied current ranging from -100 mA to 100 mA (sample #6), The contact resistance and wire resistance were not removed.

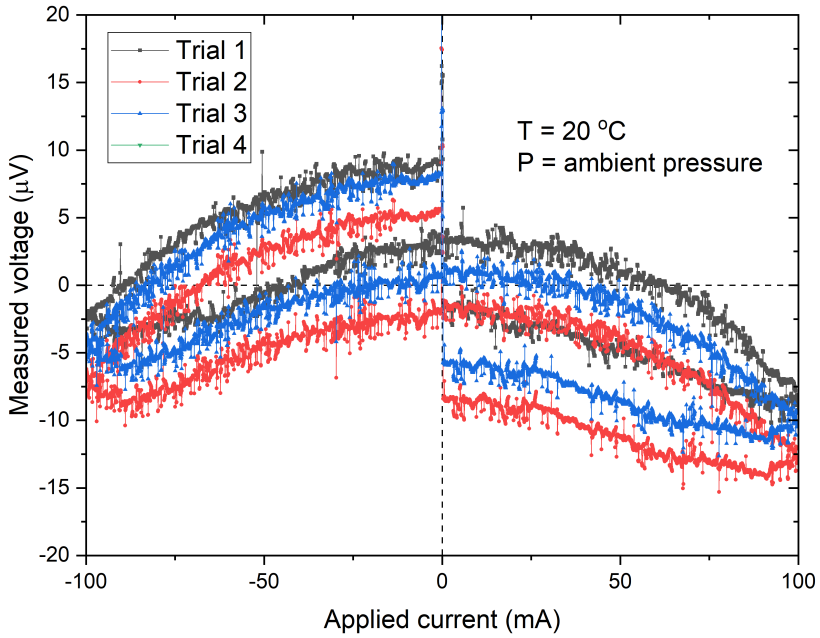

Fig. 4. Measured voltages for applied current ranging from -100 mA to 100 mA (sample #8), Semiconducting phase was included.

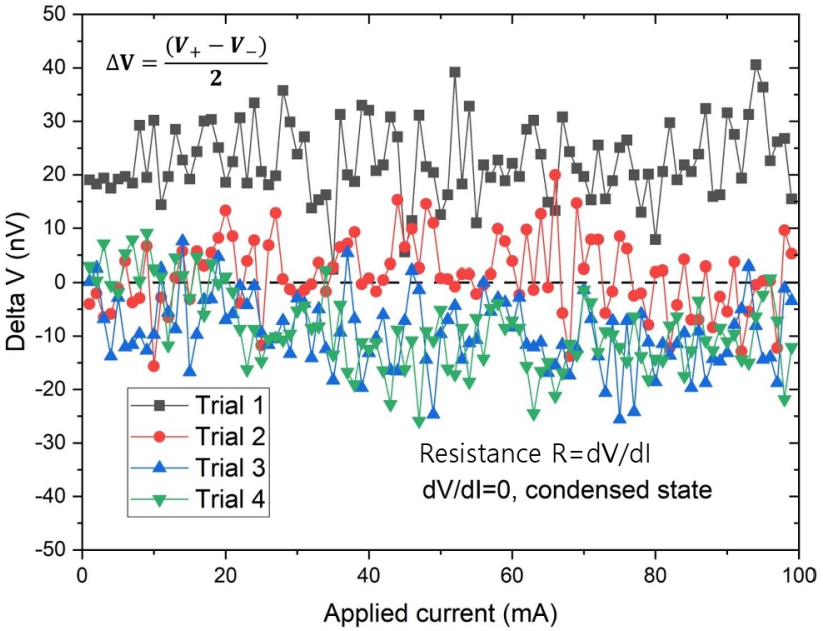

Fig. 5. Delta voltage, $V \equiv \Delta V = \frac{V_+ - V_-}{2}$ for sample #5. V_+ (or V_-) is a voltage when positive (or negative) current I_+ (or I_-) flows, respectively. Superconductivity is defined as R=0 in Resistance R=slope=dV/dI, which indicates flat with I.

IV. Measurement of the temperature dependence of resistance and phase transition
We measured the temperature dependence of samples #5 and 7. For the measurements, we utilized a ceramic-coated hot plate which uses Mica plate heater (HK Science, Model: GLHP-D). Figs. 6 and 7 show the measured voltages depending on the temperature for samples #5 and 8 when applying a current of 1 μA, respectively. The samples exhibited phase transitions at specific temperatures, clearly indicating the presence of the superconducting phase in PCPOSOS. These transitions were consistently observed. We repeatedly performed the measurement of the voltage versus temperature for sample #8 under applied current conditions of 10 and 100 mA (Fig. 8). Considering heat conduction and temperature gradient, the estimated critical temperatures are around the range of $373 \sim 400\,\mathrm{K}$. Interestingly, the temperature range of the phase transition aligns with the values provided by the original authors [7].

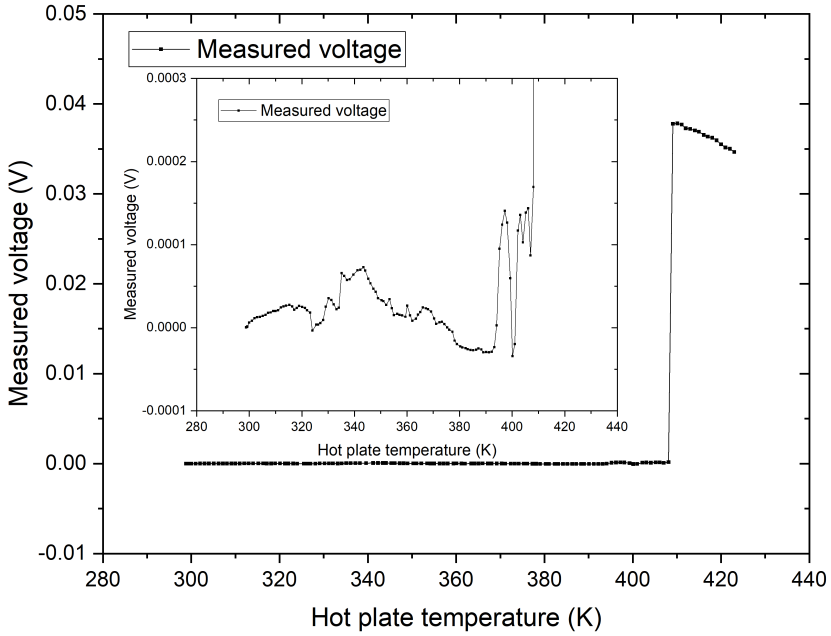

Fig. 6. Temperature dependence and phase transition of sample#5 for applied current of 1 μA. Inset shows a magnified part below on-set Tc and a noise of zero resistance.

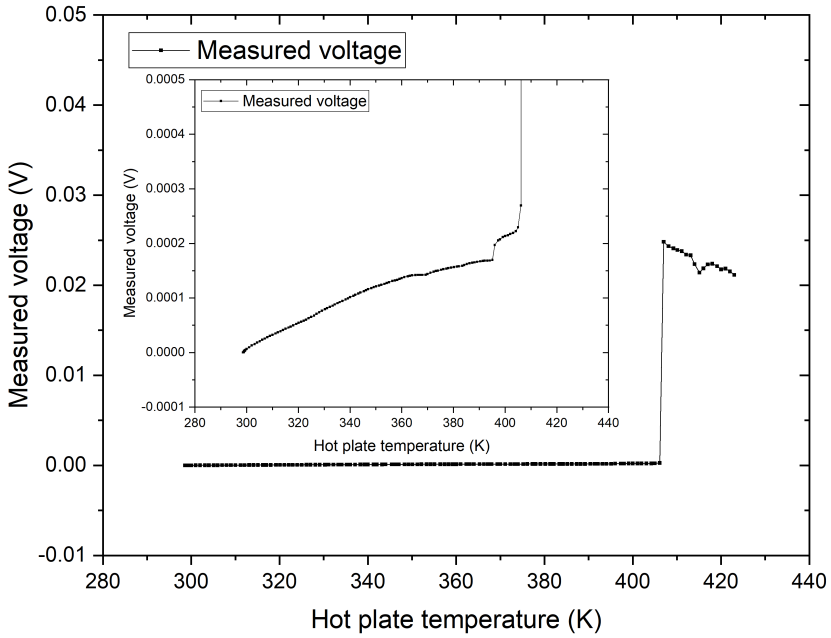

Fig. 7. Temperature dependence and phase transition of sample#8 for applied current of 1 μA. Inset shows a magnified part of on-set Tc.

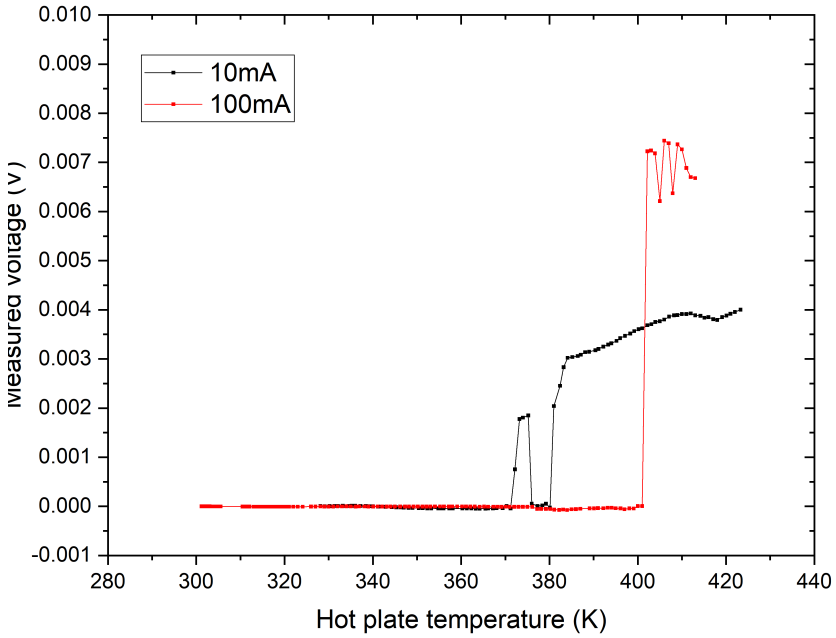

Fig. 8. Temperature dependence and phase transition of sample#8 for applied current of 10 and 100 mA.

We employed delta mode to mitigate the distortion of measured voltage. Delta mode applies a step function shaped current to correct the voltage noise. Fig. 9 shows the temperature-dependent

measured voltage of sample #5 in delta mode, V=ΔV. When viewed on a logarithmic scale, it is evident when the transition occurs at the same temperature. Despite the use of delta mode in previous transitions, distortion in the measured voltage due to increased resistance of wires and probes with temperature rise is observed. That is, what is significant in Figs. 6 to 9 is not the measured voltage values but the transition phenomenon with respect to temperature. To reiterate, when temperature is applied, the measured voltage is distorted due to the increase in temperature of the measuring device. This implies that before the transition temperature, the delta V resistance is much larger than the actual value. Similarly, when copper is measured using the same method, despite a 10K temperature change, the measured voltage increases tenfold. It is already clear fact that the resistance of copper does not increase so abruptly. This is the reason that we presented zero resistance data for applied current with fixed temperatures in Section III. The most important aspect is the transition phenomenon, which is not observed when measured with a copper plate. To accurately measure voltage, it is necessary to stabilize the measuring device for at least 2 hours at each temperature, which is not an easy task. In this study, we focused on transitions and providing raw data openly.

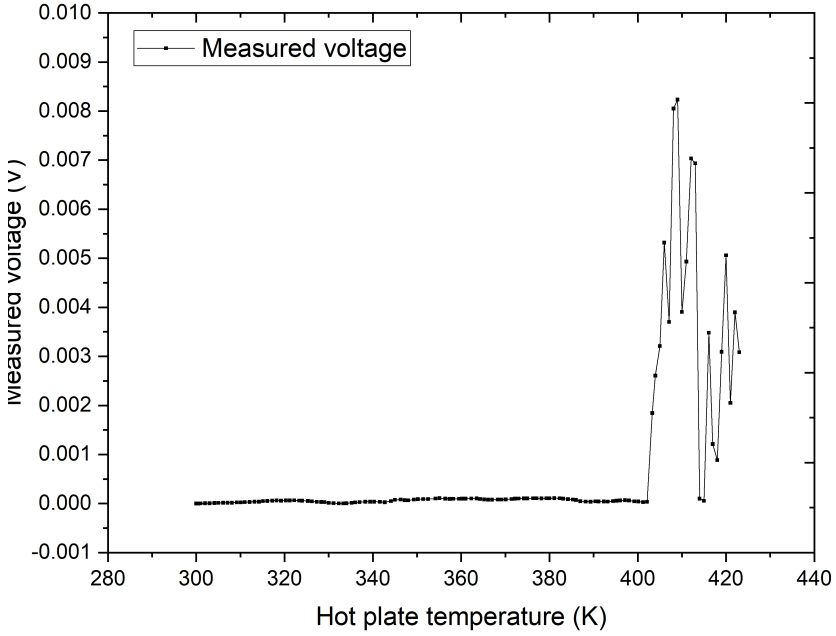

Fig. 9. Temperature dependence and phase transition of sample#5 for applied current of 10 mA, delta mode. Near 415K, the drops may be caused by heat generation of the hot plate.

V. Discussion on voltage decay phenomenon of samples

We discovered voltage decay phenomenon in the samples in voltage measurements using a power supply for DC currents (Fig. 10). In the case of sample #8, the voltage decayed exponentially at 500 mA, ultimately converging to around 300 nV. The voltage decay phenomenon is known to occur in superconducting wires or coils (percolation with temperature caused by a high current). This indicates that semiconductor phase in sample transitions to a superconducting phase. We speculate that if the channels due to the one- dimensional superconducting state have a curved shape, such a phenomenon may occur. We observed a similar phenomenon in sample #6. For sample #6, the voltage decreased ultimately converging to 500nV at 6A.

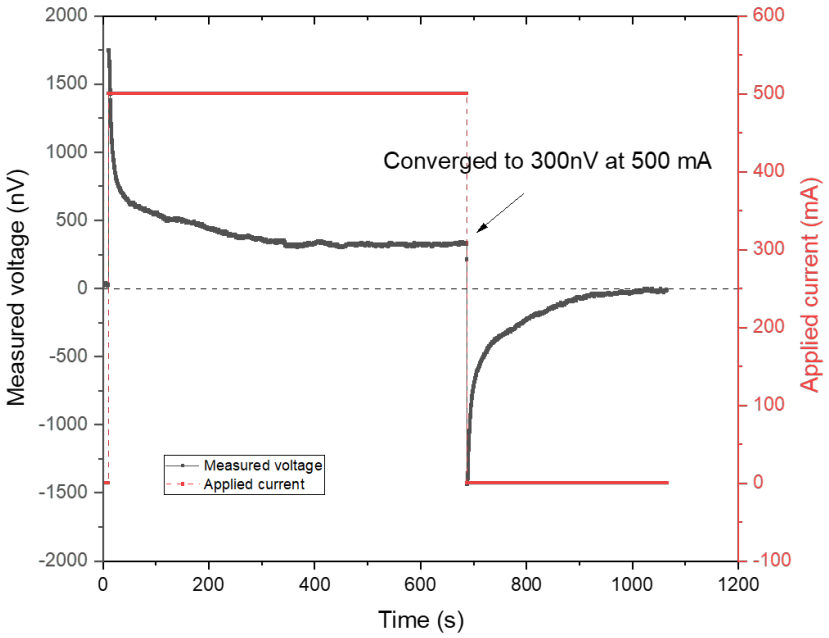

Fig. 10. Voltage decay phenomenon of sample #5 for applied current of 500 mA.The decay behavior near zero time may be caused by percolation induced by heat at 500mA. This indicates the presence of semiconducting phase in which resistance decreases with increasing temperature.

VI. Decomposing of PCPOSOS formula

A: Coper-doped lead apatite structure in reference 7

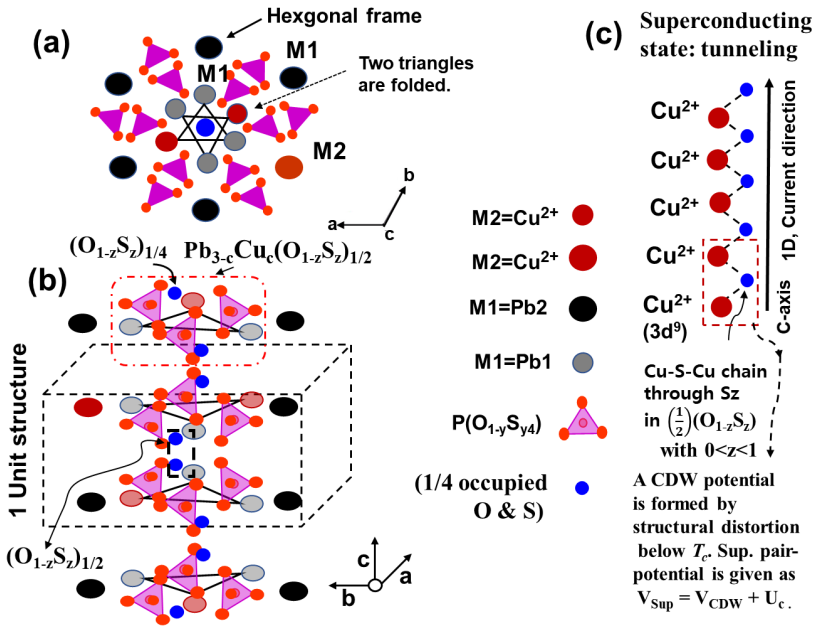

Fig. 11 Structure of PCPOSOS. (a) Top view of Cu-doped lead apatite,

$Pb_{10-x}Cu_x(P(O_{1-y}S_y)_4)_6O_{1-z}S_z$, to c-axis. Inside, hexagonal six (M1+M2)s corresponding to $(Pb_1 + Cu)$s are folded by two layers composed of $Pb_{3-x}Cu_x(O_{1-z}S_z)_{\frac{1}{2}}$ expressed as a triangle. (b) Side view of the Cu-doped lead apatite. One unit structure is also displayed. Outside frame, each layer was surrounded by six (M1+M2) atoms of the hexagonal structure at the Pb(2) position. One unit structure is composed of two folds of both outside six atoms and inside triangle one layer. Outside, the M1 four atoms structure with two atoms at each layer are formed by 6(hexagonal) x (1/3, share of one atom) x 2 (layer). In the superconducting state, layout to explain a one-dimensional superconducting chain $Cu - (S_z)_{\frac{1}{2}} - Cu$ in $Cu(O_{1-z}S_z)$ along the c-axis. The CDW is the charge-density-wave and V_{CDW}<0 is the CDW potential. V_{Sup}<0 is a potential containing the superconducting carrier. $U_c > 0$ is the critical on-site repulsive Coulomb energy in the Brinkman-Rice picture.

B: One-dimensional metal

We find a superconducting phase in the PCPOSOS structure. The lead apatite structure was given in Fig 11. structure given above [7]. When parts of Pb1 (meaning the Pb(1) site in the lead apatite cif.) and Pb2 (indicating the Pb(2) position in lead apatite cif.) sites are randomly substituted by Cu^{2+} ($3d^9$) (one hole) elements, the chemical formula of the Cu^{2+}-doped lead apatite structure is expressed as follows:

$Pb_{10-x}Cu_x(P(O_{1-y}S_y)_4)_6(O_{1-z}S_z)$
$= [Pb2_{4-a}Cu_a(P(O_{1-y}S_y)_4)_{(8/3)}]^F + [Pb1_{6-b}Cu_b(P(O_{1-y}S_y)_4)_{(10/3)}(O_{1-z}S_z)]^T$, where $a + b = x$,
$= [Pb2_{4-a}Cu_a(P(O_{1-y}S_y)_4)_{(8/3)}]^F + [Pb1_{3-c}Cu_c(P(O_{1-y}S_y)_4)_{(5/3)}(O_{1-z}S_z)_{1/2}$
$+ Pb1_{3-c}Cu_c(P(O_{1-y}S_y)_4)_{(5/3)}(O_{1-z}S_z)_{1/2}]^T$, where $c = b/2$, a and $b \neq 0$,
$= [Pb2_{4-a}Cu_a(P(O_{1-y}S_y)_4)_{(2+2/3)}]^F + [Pb1_{3-c}Cu_c(P(O_{1-y}S_y)_4)_{(1+2/3)}(O_{1-z}S_z)_{1/2}$
$+ Pb1_{3-c}Cu_c(P(O_{1-y}S_y)_4)_{(1+2/3)}(O_{1-z}S_z)_{1/2}]^T$, (1)

where F denotes the frame part, T expresses the part of the tunnel along the c-axis, and $(O_{1-z}S_z)_{1/2}$ is composed of $(O_{1-z}S_z)_{1/4}$+$(O_{1-z}S_z)_{1/4}$. This highly stable structure consists of two layers of frames with an interior region [8-10].

The metal phase originates from $Cu^{2+}(3d^9)$ with one hole substituted (Fig. 11 structure). A metal line such as $Cu^{2+}(3d^9)$–$(O_{1-z}S_z)_{1/2}$–$Cu^{2+}(3d^9)$ along the c-axis is formed. Hence, $Pb1_{3-y}Cu_y(O_{1-z}S_z)_{1/2}$ (= $(O_{1-z}S_z)_{1/4}$ + $(O_{1-z}S_z)_{1/4}$) structures are generated, and the oxygen and sulfur are located at slightly higher or lower position than the $Pb1_{3-y}Cu_y$ layer structure, (blue balls in the red-dot box in Fig.11 structure(b)). The nearest two $(O_{1-z}S_z)_{1/4}$s (blue balls) at the $(O_{1-z}S_z)_{1/4}$ position in the $(O_{1-z}S_z)_{1/2}$ of the 1-D channel, as shown in the black-dotted box of the unit structure in Fig. 11 structure(b), are generally repulsive. In the metal case, when $(O_{1-z}S_z)_{1/4}$ vibrates (the distance between $Pb1_{3-y}Cu_y$ and $(O_{1-z}S_z)_{1/4}$ expands and contracts), the other anti-vibrates (the distance contracts and expands). This indicates that $(O_{1-z}S_z)_{1/4}$ breathes, and that the average distance between $Pb1_{3-y}Cu_y$ and $(O_{1-z}S_z)_{1/4}$ is the same. Each unit has two $Pb1_{3-y}Cu_y(O_{1-z}S_z)_{1/2}$ structures (Fig.11 structure(b)).

Here, multiphases such as CuO, CuS, PbO, and PbS, exist in the $Pb1_{3-y}Cu_y(O_{1-z}S_z)_{1/2}$ structure. $Cu^{2+}O^{2-}$ has an energy gap of 1.7 eV and a monoclinic structure [11], regarded as a doped Mott insulator with one hole of $Cu^{2+}(3d^9)$. CuS, as a p-type semiconductor, has an energy gap of 1.2–2.24 eV and a hexagonal structure [12,13], referred to as a doped Mott insulator of $Cu^{2+}S^{2-}$ with one hole at $Cu^{2+}(3d^9)$. A doped Mott insulator involves an extrinsic semiconductor caused by impurity doping. Doping transforms the former of CuO_{1-z} into a ferromagnetic metal [14]. The latter CuS is changed into a metal by doping or excitation and was known to exhibit a behavior of zero resistance at a doping concentration of Ni [15]. Moreover, the insulating phase of PbS exhibited a diamagnetic

characteristic [16].

In the metal state, the unpaired hole carriers of Cu^{2+} in $Pb1_{3-y}Cu_y(3d^9)$ flow through the conduction band formed by Cu^{2+}–Cu^{2+} and $(O_{1-z}S_z)$s, combined by the Cu^{2+}s in the lower $Pb1_{3-y}Cu_y(O_{1-z}S_z)_{1/2}$ and the higher $Pb1_{3-y}Cu_y(O_{1-z}S_z)_{1/2}$, breathing along c-axis (Fig.11 structure(c)).

In the superconducting state, carriers of Cu^{2+}+$(3d^9)$s at the nearest neighbor sites between CuSs, not CuOs, form a bi-polaron in a superconducting bound state ($V_{\text{Super potential}} = V_{\text{CDW potential}} + U_c$, critical on-site Coulomb energy), where the charge-density-wave state (CDW) has the structure of long and short distances in $Pb1_{3-y}Cu_y$-$(O_{1-z}S_z)^{1/2}$ between nearest neighbor Cu sites combined with sulfur. The CDW is formed by breathing-mode distortion (stopping breath) between $(O_{1-z}S_z)$s in the $Pb1_{3-y}Cu_y(O_{1-z}S_z)^{1/2}$ structures. This is the basic concept for superconductivity arising from the BR-BCS theory[3]. Note that the bi-polaron is made of CuS rather than CuO because sulfur has a larger atomic radius than oxygen; CuS undergoes structural distortion more easily than CuO. In other words, the covalent bonding in CuS is stronger than that in CuO. Thus, $Cu^{2+}S_z$ not $Cu^{2+}O_{1-z}$ becomes a diamagnetic superconductor. Moreover, because CuO_{1-z} is ferromagnetic, it cannot form the superconducting pair because of the exchange interaction for ferromagnetism. Then, the distance between $Pb1_{3-y}Cu_y$ and $(O_{1-z}S_z)^{1/4}$ in the CDW state differs, which is attributed to a structural distortion, and the on-site Coulomb interaction, U, between carriers in the metal changes to U_c. The formation of the superconducting bound state is facilitated by the enhanced on-site Coulomb repulsive interaction, resulting from both the structural contraction (1st) at the frame of the lead apatite induced by Cu^{2+} doping and the structural distortion accompanied by volume contraction (2nd) owing to the temperature difference ($\Delta T = T_{IMT} - T_c$) at T_c. These factors contribute to superconducting condensation.

The bipolaron can tunnel through a barrier between two $Pb1_{3-y}Cu_y(O_{1-z}S_z)_{1/2}$ structures in the one-dimensional chain along the c-axis, where the Cu in the lower $Pb1_{3-y}Cu_y(O_{1-z}S_z)_{1/2}$ is connected to $(O_{1-z}S_z)_{1/2}$ and Cu in the higher $Pb1_{3-y}Cu_y(O_{1-z}S_z)_{1/2}$, (Fig.11 structure(c)).

VII. Conclusion

In this study, we have clearly showed the superconductivity of PCPOSOS. Each sample exhibited zero resistance and superconductor-conductor phase transitions, with zero resistance values and critical temperatures clearly matching the data provided by the original authors. We will release the raw data and videos of the zero resistance and temperature-dependent measurements publicly available online. Also, we will sequentially disclose XRD analysis, SQUID M vs H Meissner effect, and critical current data in future papers. Hyun-tak Kim asserts that CuS phase in PCPOSOS is a superconducting phase. A scholarly mindset entails a critical attitude. It is important to distinguish between skepticism and denial and maintain an attitude aimed at uncovering the truth. We welcome constructive discussions and questions regarding our samples and data.

Acknowledgment

We acknowledge that Quantum Energy Research Centre in South Korea for providing valuable insights and response to our inquiries regarding measurement methods.

Competing interests

Authors declare that they have no competing interests.

References

[1] H. T. Kim, S. B. Lee, S. Y. Im, S. M. An, and K. H. Auh, Abstract : Partial levitation, type-II-superconductor characteristic, at room temperature and atmospheric pressure in PCPOSOS, APS March Meeting 2024, (2024).

[2] S. M. Griffin, Origin of correlated isolated flat bands in copper-substituted lead phosphate apatite, arXiv: 2307.16892 (2023).

[3] H. T. Kim, Room-temperature-superconducting Tc driven by electron correlation, scientific report 11, 10329 (2021).

[4] H. Wang, Y. Yao, K. Shi, Y. Zhao, H. Wu, Z. Geng, S. Ye, and N. Chen, Possible Meissner effect near room temperature in copper-substituted lead apatite, arXiv: 2401.00999 (2024).

[5] H. G. Kim and D. C. Jeong, The Potential Zero-Resistance Phenomenon of the Pb-cu-P-S-O Compound and Its Synthesis Method, viXra: 2403.0040 (2024).

[6] S. B. Lee, J. H. T. Kim, S, Y. Im, S. M. An, Y. W. Kwon, and K. H. Auh, Consideration for the development of room temperature atmospheric-pressure superconductor (LK-99), J. Korean Cryst. Growth Cryst. Technol., 33(2), 61 (2023).

[7] S. B. Lee, H. T. Kim, S, Y. Im, S. M. An, and K. H. Auh, Superconductor $Pb_{10-x}Cu_x(PO_4)_6O$ showing levitation at room temperature and atmospheric pressure and mechanism, arXiv: 2307.12037 (2023).

[8] T. Baikie, M. Schreyer, F. Wei, J. S. Herrin, C. Ferraris, F. Brink, J. Topolska, R. O. Piltz, J. Price, and T. J. White, The influence of stereochemically active lone-pair electrons on crystal symmetry and twist angles in lead apatite-2H type structures, Mineralogical Magazine 78, 325 (2014).

[9] S. M. Antao and I. Dhaliwal, Lead apatites: structural variations among Pb5(BO4)3Cl with B = P (pyromorphite), As (mimetite) and V (vanadinite), J. Synchrotron Rad. 25, 214 (2018).

[10] G. Cametti, M. Nagashima,, and S. V. Churakov, Role of lone-pair electron localization in temperature-induced phase transitions in mimetite, Structural science, Crystal engineering and Materials 78, 618 (2022).

[11] Z. S. Fishman, B. Rudshteyn, Y. He, B. Liu, S. C., Mikhail Askerka, G. L. Haller, V. S. Batista, and L. D. Pfefferle, Fundamental Role of Oxygen Stoichiometry in Controlling the Band Gap and Reactivity of Cupric Oxide Nanosheets, J. Am. Chem. Soc. 138, 10978 (2016).

[12] C.J. Diliegros-Godines, D.I. Lombardero-Juarez, R. Machorro-Mejía, R. Silva González, Mou Pal, Electrical properties and spectroscopic ellipsometry studies of covellite CuS thin films deposited from non ammoniacal chemical bath, Optical Materials 91, 147 (2019).

[13] J. C. Osuwa and E. C. Mgbaja, Structural and Electrical Properties of Copper Sulfide (CuS) Thin Films doped with Mercury and Nickel impurities, IOSR Journal of Applied Physics 6, Issue 5, Version 3, 28 (2014).

[14] E. Batsaikhan, C. H. Lee, H. Hsu, C. M. Wu, J. C. Peng, M. H. Ma, S. Deleg, and W. H. Li, Lead apatitergely Enhanced Ferromagnetism in Bare CuO Nanoparticles by a Small Size Effect, ACS Omega 5, 3849 (2020).

[15] J. C. Osuwa and E. C. Mgbaja, Structural and Electrical Properties of Copper Sulfide (CuS) Thin Films doped with Mercury and Nickel impurities, IOSR Journal of Applied Physics 6, Issue 5, Version 3, 28 (2014).

[16] H. Mikhail and I. Mekkawy, Magnetic susceptibility of lead sulphide, Czechoslovak Journal of Physics B 28, 216 (1978).

APPENDIX A. RAW DATA AND MEASUREMENT VIDEO LINKS

1.zero resistance of samples, comparison with copper [raw data]:
https://docs.google.com/spreadsheets/d/1JIiuzRpCd_huiwih_y4NqJiq1u4Vb1he/edit?usp=drive_link&ouid=116167257581004355028&rtpof=true&sd=true

2.measurement video of zero resistance for sample#5 [video]:
https://youtu.be/0ldqy0XZe-s

3.raw data of this paper [raw data]:
https://docs.google.com/spreadsheets/d/1tjfgD6fo1bORhAeYMYwIkDZQjOgPSjmJ/edit?usp=sharing&ouid=116167257581004355028&rtpof=true&sd=true

4.measurement results of zero resistance for sample#6 [picture]:
https://drive.google.com/file/d/175kRGcgMc7u6uoAcRK7Y6QERmfsKoCFa/view?usp=sharing

5.measurement video of phase transition for sample#8 [video]:
https://youtu.be/OCLInsjfM9A